Int. J. Electrochem. Sci., 14 **(2019)** 875 – 885, doi: 10.20964/2019.01.76

International Journal of
ELECTROCHEMICAL
SCIENCE
www.electrochemsci.org

Short Communication

Effect of Chloride Ion Concentration on Corrosion of Q235 Steel in Sulfate-Reducing Bacteria Containing Solution

Xiaodong Zhao[1,*], *Kefeng Chen*[2,3], *Jie Yang*[1,*], *Guangfeng Xi*[4], *Haitao Tian*[1], *Qingguo Chen*[2]

[1] School of Ocean, Yantai University, Yantai 264005, China;
[2] School of Naval Architecture and Mechanical-electrical Engineering, Zhejiang Ocean University, Zhoushan 316022, China;
[3] Key Laboratory of Marine Materials and Related Technologies, Ningbo Institute of Materials Technology and Engineering, Chinese Academy of Sciences;
[4] Shandong Special Equipment Inspection Institute Lute Inspection&Testing Co. Ltd, Jinan 250100, China
[*]E-mail: danielxdzhao@aliyun.com; kittyangj@163.com

Received: 6 October 2018 / *Accepted:* 8 November 2018 / *Published:* 30 November 2018

The sedimentary water in crude oil storage tanks contains a large amount of chloride ions and microorganisms, represented by sulfate-reducing bacteria(SRB), which is the main reason for the corrosion of tank bottom. In this paper, electrochemical impedance spectroscopy(EIS) and polarization curves were used to study the effect of different chloride ion concentration on the corrosion behavior of Q235 steel in sterile solution and that containing sulphate-reducing bacteria. The results showed that the chloride ion concentration had a significant effect on the corrosion behavior of Q235 steel in SRB containing solution. With the increase of the concentration lower than 20 $g \cdot L^{-1}$, the current density of Q235 steel in SRB solution was greater than that of the sterile solution for the synergistic effect of chloride ion and SRB, and the corrosion potential shifted negatively, indicating that the microorganisms promoted the corrosion of Q235 steel. When the chloride ion concentration exceeded 20 $g \cdot L^{-1}$, the corrosion rate of Q235 steel decreased with the increase of the concentration. The self-corrosion current density was much smaller than that in the sterile solution, and the corrosion potential shifted positively, revealing that the higher chloride concentration inhibited the growth of sulfate-reducing bacteria.

Keywords: Electrochemical impedance spectroscopy (EIS), Corrosion, Sulfate-reducing bacteria (SRB), Synergistic effect

1. INTRODUCTION

Metal structures such as ships, marine equipment and oil storage tanks are extremely prone to corrosion in the marine environment. The presence of large quantities of chloride salts and different microorganisms causes significant corrosion of material and affects its performance and service life,

leading to a serious security risk [1~3]. Scholars have carried out a lot of research on the corrosion mechanism and corrosion effects of marine engineering materials, especially the process influenced by single factors, such as chloride ions, sulfide ions, single bacteria of microorganisms. For example, Allam [4] showed that with the increase of metal thickness, the film that chloride ions penetrated became thinner and the formation of chloride slowed down, which reduced the corrosion rate of the material. Robert [5] investigated the kinetics of iron dissolution in acidic chlorides by potentiostatic polarization curves, showing that at constant pH, an increase in chloride ion concentration accelerated the rate of iron dissolution. Zhang [6] analyzed the polarization curves and found that the corrosion current density of Q235 steel increased with the increasing concentration of sulfide ion and immersion time, and the extent of corrosion was aggravated. Yang [7] found that the presence of SRB in seawater accelerated the corrosion rate of carbon steel when studying the corrosion of Q235 steel in seawater containing sulfate-reducing bacteria by using corrosion potentials and polarization curves, and scanning electron microscopy showed the emergence of a large number of pitting corrosion holes.

The above studies are mostly focused on the corrosion process influenced by single factor and lack of integrated analysis of multiple factors and defections about fundamental research [8]. The result of interaction is not simply equal to the superposition of the effect caused by the single factor, while in most cases, it is greater than or less than that of the effect caused by the single factor. The sedimentary water resulted from the water in the crude oil deposited in the bottom of the tank for a long time is the main reason for the corrosion of crude oil tank bottom. The sedimentary water is composed of electrolytes including a large number of chloride, sulfide and microorganisms represented by sulfate reducing bacteria [9], leading to corrosion even perforation of the inner wall of the tubes in contact with the sedimentary water. Among the multiple factors, the concentration of chloride ion reflects the salinity of the medium. Sulfate-reducing bacteria have certain physiological requirements for salinity, and appropriate salinity is conducive to its growth. In addition, chloride ion is a living anion with small ion radius and strong penetrability, so it is easy to for it to pass through the original holes or defects on the protective film surface under the conditions of diffusion or electric field, and interact with metal to produce chloride salt. Then the following hydrolysis of the salts result in lower pH, corrosion of metals and biofilms.

In recent years, a lot of research has been carried out on the corrosion behavior of crude oil storage tanks in sedimentary water [10~13]. However, due to the different characteristics of crude oil and material of storage tanks, the impurities in sedimentary water are different. In this study, different concentration of NaCl was used to simulate the content of Cl^- in sedimentary water of bottom tank to investigate the effect of different Cl^- concentrations on the corrosion behavior of Q235 steel in sterile and sulphate-reducing bacteria containing solution.

2. EXPERIMENTAL SECTION

The chemical composition (wt. %) of the Q235 steel used in the storage tank is as follows: C 0.18, Si 0.18, Mn 0.36, P 0.016, S 0.008, Al 0.011, Fe margin. The sample was cut from a Q235 steel plate and sealed with epoxy resin leaving a square working area of $1cm^2$ exposed to the electrolyte, and

the non-working surface was weld with copper wire. Before the experiment, the working surfaces were abraded with a series of silicon carbide papers (up to 1500), and then washed with distilled water and degreased in acetone and dried. The electrode was kept in a deoxygenated chamber, sterilising by ultraviolet lamp for 30 min prior to testing.

The sulfate-reducing bacteria was provided by Chinese Academy of Sciences, Institute of Oceanology. A modified Postgate's C medium, which contained 0.5 g KH_2PO_4, 1.0 g NH_4Cl, 0.06 g $CaCl_2·6H_2O$, 0.06 g $MgSO_4·7H_2O$, 6 ml 70% sodium lactate, 1 g yeast extract and 0.3 g sodium citrate in 1 L seawater, was used for the enrichment culture. The medium was deoxygenated by purging high purity nitrogen for 20 min, and autoclaved at 121℃. A sterile 0.004 $g·L^{-1}$ $FeSO_4·7H_2O$ was then added. With reference to the chloride ion concentration in the sedimentary water at the bottom of the crude oil tank in natural environment, NaCl was added to prepare the PGC solution containing 0, 5, 10, 20 and 30 $g·L^{-1}$ Cl^-, and the pH was adjusted to 6.5 with 0.01 $mol·L^{-1}$ NaOH, serving as sterile solution. The PGC solution was infused a modified medium with inoculated SRB, which was stirred adequately with a sterile glass stick and deposited for 24 h, serving as experimental solution containing SRB.

The experiments were performed in a classical three-electrode cell, with a platinum electrode used as the counter electrode, and a saturated calomel electrode (SCE) as the reference electrode. All tests were operated using an EG&G Parstat 2273 electrochemical system. Electrochemical impedance spectroscopy was performed in the frequency range of 10MHz~100KHz and the amplitude of the sinusoidal voltage signal was 10mV. The polarization curve was tested in a scanning range of -350mV to +350mV at a scanning rate of 0.333 mV/s.

3. RESULTS AND DISCUSSION

3.1 The corrosion of Q235 steel in sterile solution with different Cl^- concentrations

Fig.1 shows the Nyquist and Bode diagrams of the Q235 steel in different Cl^- concentration solutions.

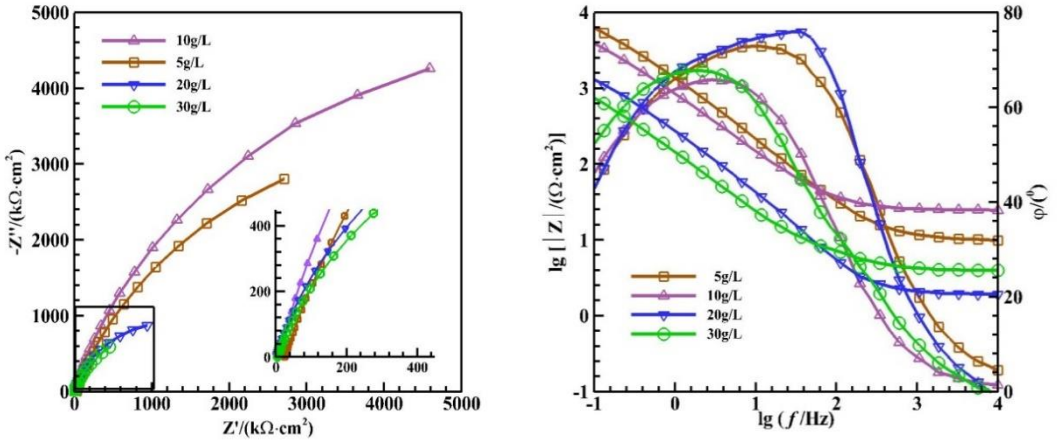

(a) Nyquist diagram (b) Bode diagram

Figure 1. Nyquist and Bode diagrams of the Q235 steel in different Cl^- concentration solutions

In the experimental concentration range of Cl^-, as shown in Fig.1, the Q235 steel exhibited semicircular arcs at different concentrations of chloride ions, which had the characteristic of capacitance due to the presence of the corrosion product layer on the steel surface [14]. The capacitance arcs were irregular due to the "dispersion effect" caused by the heterogeneity of the film on the electrode surface [15].

In addition, it was obvious that the capacitive arc radius was the largest when the chloride ion concentration was 10 $g \cdot L^{-1}$, indicating that the polarization resistance value was the largest and the corrosion rate was relatively small. It was because that at lower concentration of chloride ions, the generation of corrosion product layer on the Q235 steel surface had a temporary protective effect. With the increase of chloride ion concentration, the arc radius of capacitance decreased significantly, indicating that the corrosion rate of Q235 steel was increasing due to the penetration of chloride ions into the non-uniform corrosion product layer on the working electrode surface [16].

Using Zsimpwin software the EIS spectra are fitted with the equivalent circuit (Fig.2) and the fitting parameters obtained are shown in Tab.1. In the equivalent circuit model, R_s represents an electrolyte resistance, Q_c represents the non-ideal capacitance of the corrosion product layer, R_c represents the corrosion product layer resistance, Q_{dl} represents the double layer capacitance, and R_{ct} represents the charge transfer resistance. The fitting parameters in Tab.1 obtained according to the equivalent circuit showed that the corrosion product layer resistance reached it maximum value of 3062 $k\Omega \cdot cm^2$ at the chloride ion concentration of 10$g \cdot L^{-1}$, representing an maximum of corrosion resistance until the concentration is exceeded.

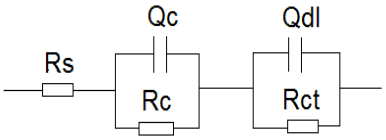

Figure 2. The equivalent circuit model used to fit the EIS experimental data for Q235 steel in solutions with different Cl^- concentration

Table 1. Fitting parameters derived from equivalent circuit model in Fig.2

c(Cl^-) $g \cdot L^{-1}$	R_s $\Omega \cdot cm^2$	$Q_c \times 10^{-4}$ （uF/cm^2） $Hz^{1-n}{}_1$	n_1	R_c $k\Omega \cdot cm^2$	$Q_{dl} \times 10^{-4}$ （uF/cm^2） $Hz^{1-n}{}_2$	n_2	R_{ct} $k\Omega \cdot cm^2$
5	23.86	4.01	0.76	823.9	3.88	0.70	5865
10	9.77	1.89	0.82	3062	1.25	0.78	8591
20	1.56	3.78	0.93	204.3	5.02	0.71	1755
30	1.12	2.27	1	2.71	2.35	0.773	1532

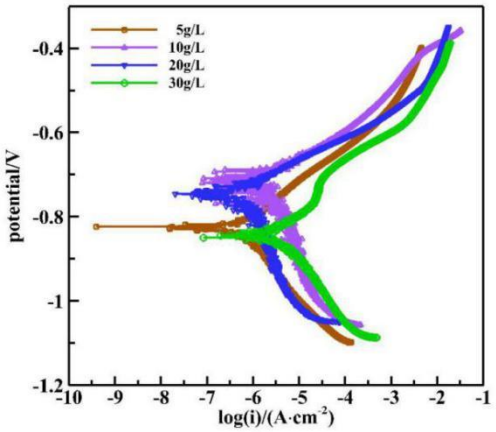

Figure 3. Polarization curves of Q235 steel in solutions with different Cl^- concentration

Fig.3 showed the potentiodynamic polarization curves of Q235 steel in solutions with different Cl^- concentration. The relevant electrochemical corrosion parameters were obtained using the C-view software for the Tafel plots of the polarization curves, shown in Tab.2. As shown in Fig.3, in all solutions with different chloride ion concentrations except the value of 30g·L^{-1}, the slope of the cathodic polarization curves was significantly larger than that of the anodic polarization curves. The anodes were in active dissolved state without passivation, indicating that the corrosion reaction was controlled by the cathode reaction. But when the value of chloride concentration was 30g·L^{-1}, we could see that the value of anode slope (197 mV·dec^{-1}) slightly larger than the value of cathodic slope (171 mV·dec^{-1}), indicating the corrosion reaction was a mixed control reaction at the concentration. The behavior might be due to the high concentration of chloride ions in the solution induced corrosion of the Q235 steel and the resulting corrosion products heavily deposited on the surface as well as the rapid consumption of dissolved oxygen in the solution.

Table 2. Corrosion parameters of Q235 steel in solutions with different Cl^- concentration

c(Cl^-, g·L^{-1})	E_{corr}（V,vs.SCE）	i_{corr}（μA·cm^{-2}）	β_a（mV·dec^{-1}）	-β_c（mV·dec^{-1}）
5	-0.811	2.521	57	84
10	-0.717	3.364	72	237
20	-0.761	3.529	72	104
30	-0.844	3.687	197	171

According to the corrosion parameters in Tab.2, when the chloride ion concentration was relatively low, the corrosion current density as well as the corrosion rate of carbon steel Q235 were small. It was probably because that lower chloride ion concentration was not enough to cause rapid corrosion of Q235 steel. The self-corrosion current density increased sharply from 2.521μA·cm^{-2} to 3.364μA·cm^{-2} with the increase of the chloride ion concentration from 5 to 10 g·L^{-1}. When the chloride ion concentration was higher than 10 g·L^{-1}, the self-corrosion current density increased with the increase

of chloride ion concentration and eventually it tended to be stable. This is consistent with the EIS result discussed above.

3.2 The corrosion of Q235 steel in SRB-containing solution with different Cl^- concentrations

Fig.4 shows the EIS diagrams of the Q235 steel in SRB-containing solution with different Cl^- concentrations.

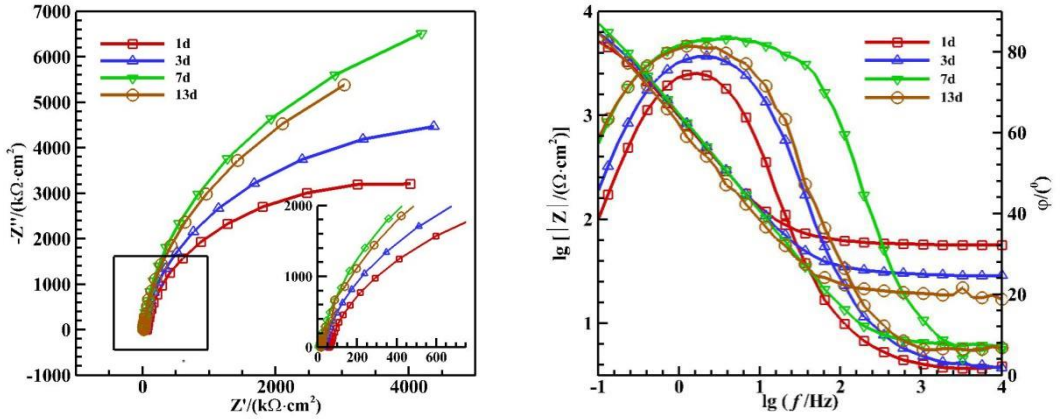

(a) 0 $g \cdot L^{-1}$ Cl^-

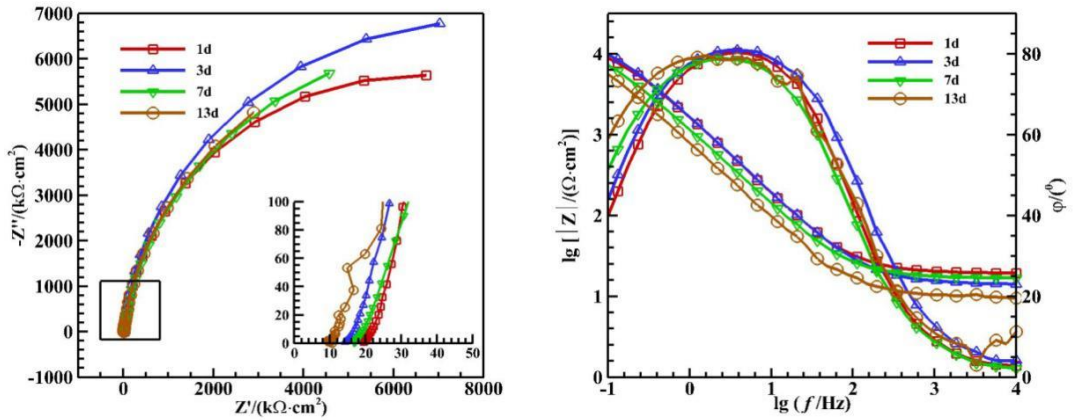

(b) 5 $g \cdot L^{-1}$ Cl^-

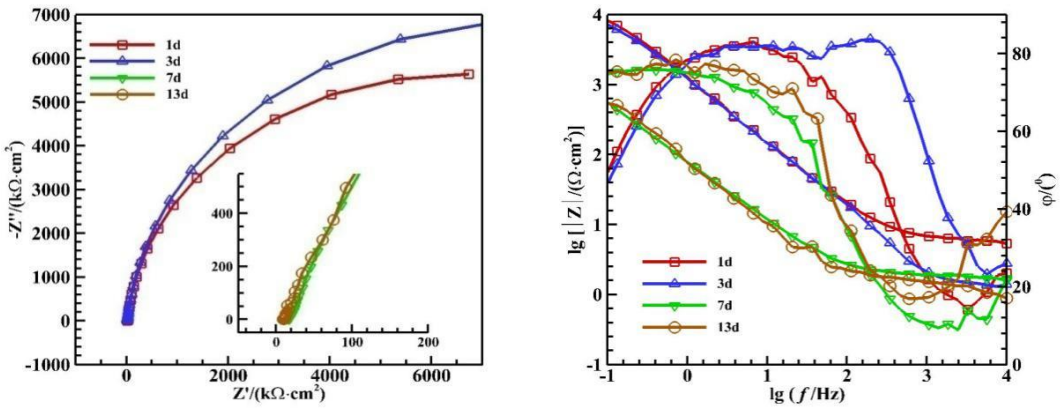

(c) 10 $g \cdot L^{-1}$ Cl^-

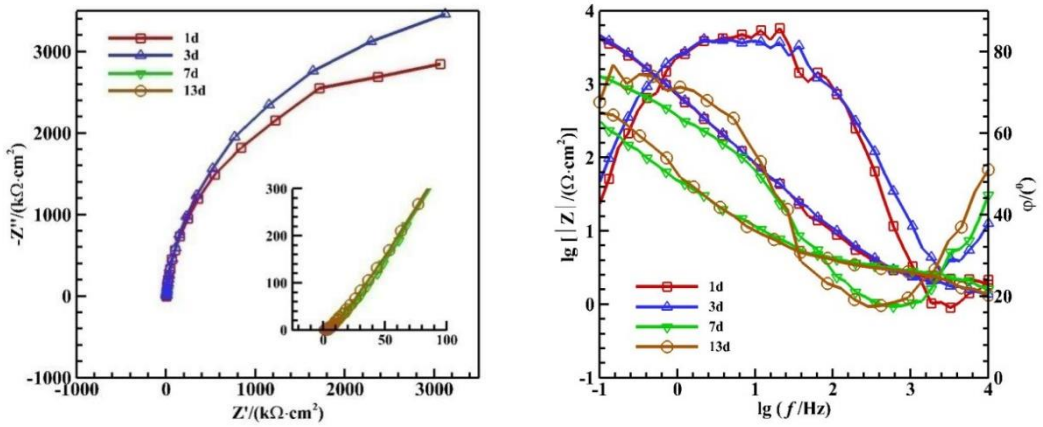

(d) 20 g·L^{-1} Cl$^-$

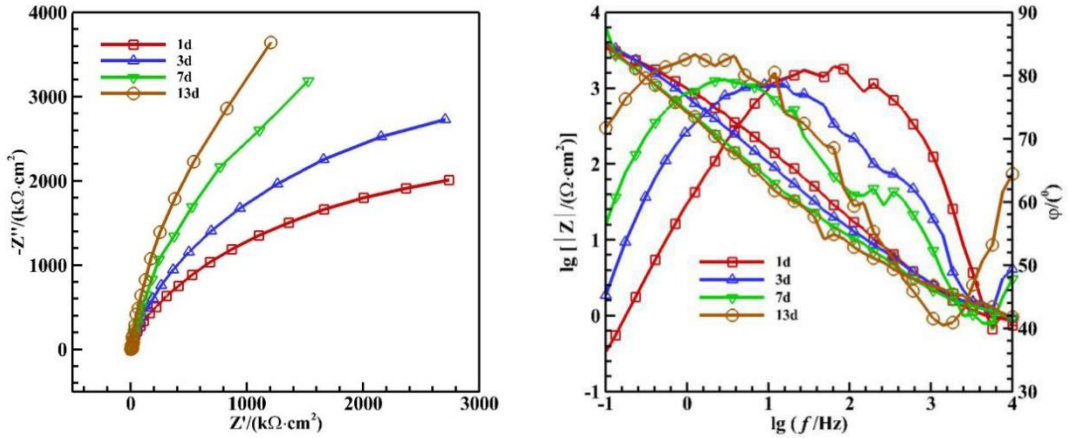

(e) 30 g·L^{-1} Cl$^-$

Figure 4. EIS diagrams of the Q235 steel in SRB-containing solution with different Cl^- concentrations.

As is seen from Fig.4 (a) and (b), the capacitive radius increased in 7 days and then decreased over time, showing that when the concentration of chloride ion was relatively small, the steel substrate was not prone to corrode due to the generation of FeS resulted from the reaction of H_2S produced by the proliferation and growth of SRB, and Fe^{2+} in solution.

With the extension of time, the composition of the original protective film gradually transformed from FeS to $Fe_{1-x}S$ with large grain size and incomplete crystal lattice, which fell off easily then leaving the substrate re-exposed to the corrosive medium and thus accelerating the corrosion [17~18]. However, as is seen from the Nyquist plots in Fig.4(a) and (b), the capacitive arc radius increased as the chloride ion concentration changed from 0 to 5 g·L^{-1}. It was presumed that at low concentration, Cl^- might promote the growth of SRB to some extent, so the corrosion product layer had a good protective effect on the substrate. It is seen from Fig.4(c) that the capacitive arc radius after immersion for 7d decreased greatly compared with that of 1d and 3d, and the corrosion might be rapidly accelerated due to the transformation of the corrosion product layer. In Fig.4(d), the capacitive arc radius increased first and then decreased rapidly. The higher Cl^- concentration may accelerated the corrosion after the corrosion

product layer was damaged. In Fig.4(e), the capacitive arc radius gradually increased and the corrosion rate decreased. It was because that the high chloride ion concentration inhibited the growth of SRB and the steel substrate was always under protection of the corrosion product layer during the testing period.

Fig.5 shows the polarization curves of Q235 steel after immersion in SRB-containing medium with different chloride ion concentration for 13 days.

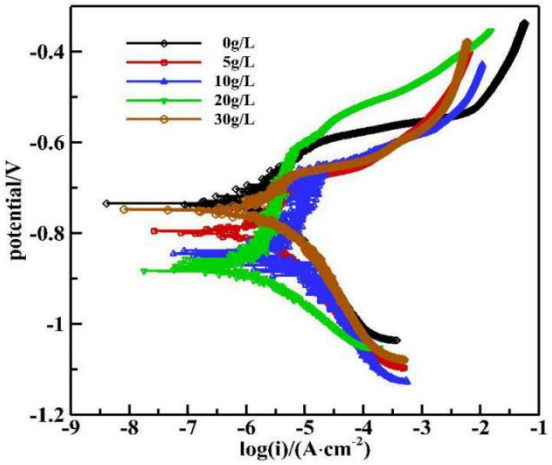

Figure 5. Polarization curves of Q235 steel after immersion in SRB-containing medium with different chloride ion concentration for 13 days.

Table 3. Corrosion parameters of Q235 steel in SRB-containing medium with different Cl^- concentration

c(Cl^- , g·L^{-1})	i_{corr}(A·cm^{-2})×10^{-7}	E_{corr}（V,vs.SCE）
0	1.114	-0.744
5	1.283	-0.796
10	3.302	-0.828
20	21.179	-0.867
30	4.639	-0.726

The C-view software is used to fit the polarization curves in Tafel zone and the electrochemical parameters are listed in Tab.3. As shown in Fig.5, when the added chloride ion concentration was zero, the self-corrosion potential was the most positive. With the increase of chloride ion concentration until 20 g·L^{-1}, the corrosion potential decreased from -0.744V to -0.867V, and the corrosion current density increased, indicating that the corrosion tendency gradually increased and reached the maximum value at concentration of 20 g·L^{-1}. This was due to the fact that with the increase of chloride ion concentration in the solution, the growth of SRB was promoted to a certain extent, and its metabolite, sulfide, had a depolarization function, resulting in the acceleration of the corrosion rate. In addition, the increase of chloride ion concentration was also one of the reasons for the accelerated corrosion, since Cl^- was an extremely depassivating agent [19~20], which was easily adsorbed on the electrode surface to promote the detachment of the surface membrane and penetrated the substrate to cause corrosion. Subsequently, the corrosion current density decreased with the increase of chloride ion concentration, which was due

to the high concentration of chloride ion against the reproductive growth of SRB. While the high concentration of chloride ion also led to the reduction of dissolved oxygen in solution and also the corrosion rate. This was consistent with the results of the impedance diagram above.

3.3 Discussion

According to the study of Pan [21], only considering the effect of chloride ion concentration on the corrosion of Q235 steel, the change of surface film capacitance of Q235 steel was attributed to the increase of film thickness during its immersion. The initial deposition of chloride ion had a significant influence on the film thickness. With the increase of the concentration of chloride ion, it was easy to penetrate the membrane into the interior for its small radius. Uneven film thickness and "pitting corrosion" occurred on the steel surface after a series of reactions.

Moreover, the electrochemical parameters obtained from the equivalent circuit in Tab.1 showed that the fitted capacitance fluctuated with the variation of chloride ion concentration rather than changed monotonically, indicating that the effect of different chloride ion concentrations on the corrosion of steel varied as chloride ions at low concentration could not penetrate the metal surface [22]. In addition, a biofilm was formed on the Q235 steel surface when the sample was immersed in a culture medium containing sulfate-reducing bacteria (SRB). Negative charged biofilm easily excluded anions such as sulfate ions from it [23]. SRB utilized sulfate ions as terminal electron acceptors and organic materials as carbon sources. During the metabolic process, sulfate ions were reduced to sulfide ions. Sulfide ions reacted with ferrous ions to form FeS adsorbed on the inner surface of the biofilm.

A small amount of FeS and ferrous hydroxide generated by the reaction of other ferrous ions with hydroxyl ions were adsorbed on the biofilm micropores [24, 25], resulting in localized corrosion as "pitting". Generally pitting is caused by two mechanisms: one is localized corrosion caused by SRB adsorption on the surface of the carbon steel. As the hydrogen sulfide produced in the metabolic process of SRB is corrosive to metal materials, leading to the dissolution of the metal and then the occurrence of pitting. The other is that the corrosive micro-cells in a region form a micro-battery and pitting occurs in the anode area. A series of reactions will take place as follows:

Anodic reaction

$$Fe \rightarrow Fe^{2+} + 2e^{-} \quad (1)$$

Cathodic reaction

$$H^{+} + e^{-} \rightarrow H \quad (2)$$

SRB consumption reaction

$$SO_4^{2-} + 8H \rightarrow S^{2-} + 4H_2O \quad (3)$$

Corrosion product (1)

$$Fe^{2+} + S^{2-} \rightarrow FeS \quad (4)$$

Corrosion product (2)

$$Fe^{2+} + 2OH^{-} \rightarrow Fe(OH)_2 \quad (5)$$

Ionization of water balance

$$H_2O \rightarrow H^{+} + OH^{-} \quad (6)$$

The total reaction equation

$$4Fe + SO_4^{2-} + 4H_2O \rightarrow 3Fe(OH)_2 + FeS + OH^{-} \quad (7)$$

4. CONCLUSION

In sterile solutions, changes of chloride ion concentration could affect the corrosion rate of Q235 steel. At the chloride ion concentration of 10 $g \cdot L^{-1}$, the self-corrosion current density reached 3.364 $\mu A \cdot cm^{-2}$, and the corrosion resistance at the time was the strongest, for the corrosion products on the steel surface protected the substrate to a certain extent. With the increase of chloride ion concentration, the self-corrosion current density reached 3.687 $\mu A \cdot cm^{-2}$ at the concentration of 30 $g \cdot L^{-1}$ for the product layer was penetrated by chloride ions, causing local "pitting" and accelerating the corrosion rate.

In SRB-containing solutions, the effect on the corrosion of steel varied with different additive amount of chloride ions, which was related to the structure of the corrosion product layer attached to steel surface and the metabolites of SRB. SRB and chloride ions at certain concentration had an synergistic effect on the corrosion of Q235 steel. When the chloride ion concentration was too high, the growth of SRB was inhibited while the oxygen content of the solution was reduced, thus reducing the corrosion tendency of the Q235 steel.

ACKNOWLEDGMENTS
This research was supported by Foundation of Key Laboratory of Marine Materials and Related Technologies, Ningbo Institute of Materials Technology and Engineering, Chinese Academy of Sciences (Grant No.2017Z01). The support from Scientific Research Foundation of Yantai University (Grant No.HX17B38) is also gratefully acknowledged.

References

1. B.J. Little, P.A. Wagner and F. Mansfeld, *Microbiologically Influenced Corrosion*, (2008) Springer London, U. K.
2. X. Zhao, J. Duan and B. Hou, *Can. Metall. Quart.*, 53(2014)450.
3. T.J. Hakkarainen, *Mater. Corros.*, 54(2015)503.
4. I.M. Allam and J. S. Arlow, *Corros. Sci.*, 32(1991)417.
5. R.J. Chin and K. Nobe, *J. Electrochem. Soc.*, 119(1972)1457.
6. M. Zhang, C. Chen and J. Li, *Surf. Technol.*, 44(2015)86.
7. Z.Q. Yang, *J. South. China. Univ. Technol.*, 37(2009)135.
8. M.M. El-Naggar, *Appl. Surf. Sci.*, 252(2006)6179.
9. T.A. Syafaat and M.C. Ismail, Microbiologically influenced corrosion (MIC) of storage tank bottom plates, *Scientific Conference of Microscopy Society Malaysia*, Malaysia, 2015, 315.
10. H. Bi, D. Hu and Z. Li, *Int. J. Electrochem. Sc.*, 10(2015)6946.
11. G.Z. Li, L.H. Chen and Y. Zhang, *Corros. Prot.*, 38(2017)129.
12. S. Math, T. K. Adelakin and D. Lindemuth, External corrosion protection of underside bottom of above ground storage tank using vaporized corrosion inhibitors, N*ace Corrosion*, New Orleans, U.S.A., 2017, 1.
13. H. Bi, H. Wang and Z. Li, *Corros. Sci. Prot. Techn.*, 29(2017)381.
14. C. Cao and J. Zhang, *An Introduction to Electrochemical Impedance Spectroscopy*, Science Press, (2002)Beijing, China.
15. A. Ghosh, B. Leonard and F. Sadeghi, *Wear.*, 307(2013)87.
16. J. Wang, Research of pitting corrosion behavior in the environment of crude oil storage tank bottom,

China University of Petroleum(East China), (2014)Qingdao, China.
17. V. E. Pogulyai and I. Y. Mikhai, *Zarodsk Lab*, 31(1965)764.
18. V. E. Pogulyai and A. L. Kuz'min, *Chem. Petro. Eng.*, 7(1971)506.
19. I. B. Beech and J. Sunner, *Current opinion in Biotechnology*, 15(2004)181.
20. L. Niu, Effect of calcinedhydrotalcite(CLDE) on the corrosion of rebar by chloride, *Beijing University of Chemical Technology*, (2010)Beijing, China.
21. J. Pan, C. Leygraf and R. F. A. Jargelius-Pettersson, *Oxid. Met.*, 50(1998)431.
22. Y. Ma, Y. Li and F. Wang, *Corros. Sci.*, 51(2009)997.
23. B. C. Syrett and S. S. Wing, *Corrosion.*, 36(1980)73.
24. J. E. G. González and A. F. J. H. Santana, *Corros. Sci.*, 40(1998)2141.
25. X. Sheng, Y. P. Ting and S. O. Pehkonen *Corros. Sci.*, 49(2007)2159.